ACS OMEGA

http://pubs.acs.org/journal/acsodf

Article

Biocompatibility and Surface Roughness of Different Sustainable Dental Composite Blocks: Comprehensive In Vitro Study

Soha A. Hassan, Marwa Beleidy, and Yasmine Alaa El-din*

Cite This: *ACS Omega* 2022, 7, 34258−34267

Read Online

ACCESS | Metrics & More | Article Recommendations

ABSTRACT: The study purposed to investigate the biocompatibility and sustainability of two computer-aided design/computer-aided manufacturing (CAD/CAM) resin-based composites compared to a resin-modified ceramic in terms of surface roughness, biofilm formation, cytotoxicity, genotoxicity, and cellular changes observed under transmission electron microscopy (TEM). Three CAD/CAM blocks were used, two resin-based composites [Brilliant Crios (BC) and Cerasmart, (CS) and one hybrid ceramic (Vita Enamic (EN)]. Each block was sectioned into 10 × 12 × 2 mm specimens, followed by finishing and polishing. Each specimen was evaluated for surface roughness using 3D optical profilometry and scanned by scanning electron microscopy. Biofilm formation and its relation to surface roughness have been investigated for all tested materials. A Hep-2 cell line was used to investigate the viability through MTT assay. The cytotoxicity of the materials was measured at 24, 48, and 168 h. The activity of P53, caspase 3, and cytochrome *C* was evaluated to detect the genotoxicity of different groups, followed by TEM tracking of the cellular changes. Statistical analysis was implemented by utilizing a one-way analysis of variance test. The significance was set at $P \leq 0.05$. With regard to the surface roughness, no statistically significant differences were shown between groups. BC possessed the highest biofilm formation value, followed by EN and CS, with no significance between them. No correlation between surface roughness of tested materials and biofilm formation was shown. Considering viability, the highest values were recorded for EN, whereas BC showed the lowest values. P53-fold changes in EN were significantly the lowest, indicating less genotoxicity. Within the current study's limitations, BC showed the highest biofilm formation. However, no significant surface roughness difference or correlation with biofilm formation was observed in tested materials. EN showed the lowest cytotoxicity and the highest viability. EN revealed the best compatibility performance among tested materials. On the contrary, the BC exhibited fewer preferences.

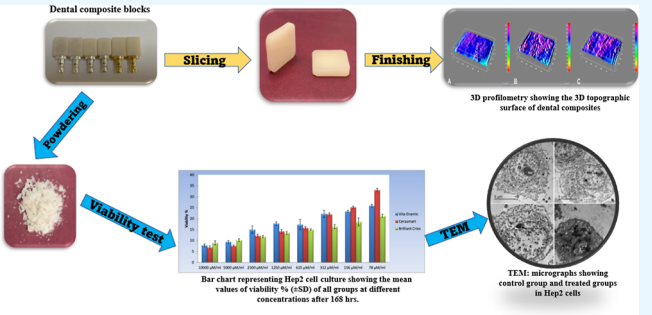

INTRODUCTION

The development of new generations of dental computer-aided design/computer-aided manufacturing (CAD/CAM) resin-modified ceramic and resin-based composite blocks has widespread uses. Their application in conservative, esthetic, and long-lasting restorations as an alternative to ceramics is currently used in dental procedures.[1] The improvement in the structure of these materials during past years enhances their mechanical and aesthetic properties. According to microstructure and fabrication techniques, these CAD/CAM materials can be classified into two groups: (i) polymer-infiltrated ceramic networks (PICNs) and (ii) ceramic particle-filled composites with dispersed fillers (zirconia, silica, and barium glass).[2]

One newly developed PICN material is Vita Enamic (EN) (Vita Zahnfabrik H. Rauter, Bad Säckingen, Germany), a hybrid ceramic. It comprises an 86% by weight feldspathic ceramic network incorporated with a polymer network (14% by weight), resulting in a suitable material for dental prosthetic restorations on natural teeth and implants due to showing the optimistic features of both ceramics and composite resins.[3,4]

Cerasmart (CS) is a high-density nanoparticle-filled composite resin with a filler particle content of 71% by weight.[5] It is regarded as a one-of-a-kind dental material that integrates the best features of high-strength ceramics and composites. This material guarantees high strength, a high degree of flexibility, breaking energy, and the best marginal integrity. Furthermore, Brilliant Crios (BC) is a 70% glass and amorphous silica-reinforced resin block.[6] The material blends the innovative submicron hybrid composite material benefits combining with those of the CAD/CAM technology for

Received: June 15, 2022
Accepted: September 6, 2022
Published: September 15, 2022

Table 1. Chemical Composition of the Tested Materials[a]

material	manufacturer	type	shade	composition		batch no.
				matrix	fillers	
EN	VITA Zahnfabrik, Bad Säckingen, Germany	hybrid ceramic PICN, HT/HP	1M1-HT	UDMA, TEGDMA (14% wt 25% v/v)	feldspar ceramic enriched with aluminum oxide (75% v/v), (86% wt)	LOT: 56802
CS	GC Dental Products Europe, Leuven, Belgium	resin composite CAD/CAM blocks	A1-HT	bis-MEPP, UDMA, DMA	silica (20 nm); barium glass (300 nm) (71% v/v)	LOT: 1610051
BC	Coltene AG, Altstätten, Switzerland	resin composite CAD/CAM blocks	A1-HT	cross-linked bis-GMA, bis-EMA, UDMA, TEGDMA	amorphous SiO_2 (<20 nm), barium glass (<1 nm), inorganic pigments: ferrous oxide or titanium dioxide	LOT: I09010

[a]Bis-EMA, bisphenol A ethoxylate dimethacrylate; Bis-GMA, bisphenol A-glycidyl dimethacrylate; DMA, *N*,*N*-dimethylacrylamide; HP, high pressure; HT, high temperature; PICN, polymer-infiltrated ceramic network material; TEGDMA, triethylene glycol dimethacrylate; UDMA, urethane dimethacrylate; and Bis- MEPP:2,2-Bis (4-methacryloxypolyethoxyphenyl) propane.

aesthetically pleasing, reliable, and quickly processed restorations without the need for a separating firing process.[7]

Dental materials' biocompatibility, aesthetic qualities, and mechanical properties are compulsory considerations for dental clinicians, especially in long-term treatment strategies.[8−10] For a better selection of suitable materials in the clinical practice, the microstructure, surface roughness, mechanical properties, interactions with the oral environment, and their ability to retain biofilm should all be well recognized.[11]

Because of incomplete polymerization and instability in the humid oral environment, resin-based materials used in prosthetic dentistry frequently have cytotoxic properties.[12] Assessment of biocompatibility is a mandatory step in the cytotoxicity of resin-based materials. Genotoxicity is also an important factor that evaluates the capacity of these materials to produce molecular DNA damage on cells. Assessment of genotoxicity of dental materials is essential for determining the health dangers due to an evidenced link between genetic damage and carcinogenesis.[13]

Cell culture techniques are a powerful tool for assessing the material's cytotoxicity in vitro. Cell culture research is commonly used to investigate their composition, structure, and elutes.[14,15] The advantages of using in vitro tests are reducing the use of experimental animals, the possibility of repeating the experiment easily, and several tests can be implemented with comparatively small sample size. The Hep-2 cell line of laryngeal carcinoma is a suitable experimental model for cytotoxicity and genotoxicity evaluation.[16] In addition to the previously mentioned advantages, the Hep-2 cell line was chosen because of its availability, stable phenotype, infinite lifespan, and ease of handling.[17]

However, little is known about the indirect composites regarding bacterial adhesion (biofilm formation) related to surface roughness and biocompatibility. This comprehensive study assessed and compared three different CAD/CAM materials regarding surface roughness, biofilm formation, cytotoxicity, and genotoxicity.

MATERIALS AND METHODS

Sample Size Calculation. The viability % after 7 days was used as the primary outcome for power analysis. Following Aydin N et al.'s study results,[18] the mean values were 91.2, 71.4, and 102 for EN, CS, and BC, respectively, with 12.67 as effect size (f). Using 5% alpha (α) level and 20% beta (β) level, the minimum estimated sample size was a total of six specimens (two specimens per group). This was increased to 10 specimens per group; three for surface roughness and biofilm formation testing, five for cytotoxicity assay, and two for qualitative scanning electron microscopy (SEM) evaluation. Statistical power analysis software (G*Power v3.1.9.2, Heinrich−Heine−Universität, Düsseldorf, Germany) was applied for sample size calculation. The Research Ethics Committee, Faculty of Dentistry, October 6 University approved this study (approval no.: RECO6U/17-2022).

Specimens' Preparation. Three CAD/CAM materials were tested: one PICN block (EN, Zahnfabrik, Bad Säckingen, Germany) and two resin-based composite blocks (RBCs) (BC, Coltene, Altstätten, Switzerland and CS, GC Dental Products Europe, Leuven, Belgium), as shown in Table 1. Through a diamond blade (MK 303, MK diamond, CA, USA) mounted on a saw (Isomet 1000 Precision Saw: Buehler Co., IL, USA) under continuous water irrigation, each CAD/CAM block was sectioned into 10 × 12 × 2 mm specimen.

Surfaces of each specimen were ground on a grinding machine (Jean Wirtz TG 250, Dusseldorf, Germany) at 200 rpm gradually up to 1200 grit silicon carbide abrasive papers (Apex S system, Buehler, Lake Bluff, IL, USA) under water cooling (50 mL/min). Then, the surfaces were polished for 60 s using diamond grit polishing discs (EVE Diapol, EVE Emst Vetter GmbH, Germany) according to manufacturer instructions.[19] First, blue discs for removing and shaping; second, pink discs for smoothening; and third, gray discs for shiny polishing. A diamond polishing paste (Renfert Polish hybrid materials; Renfert GmbH Co., Hilzingen, Germany) was rubbed using a Buff disc (Super Snap Buff Discs; Shofu Inc., Quioto, Japan). A single operator completed the polishing procedures using a blue band (1:1) contra-angle handpiece (KaVo GENTLE power LUX 20LP; KaVo Dental GmbH) connected with an adjusted and monitored micromotor. Then, the specimens were ultrasonically cleaned (Minisonic, İntersonik, Turkey) in distilled water for 10 min and air-dried. For cell culture, specimens were ground, powdered, and then weighed to suit the cell culture process.

Surface Roughness Analysis. The surface topography of all tested specimens was assessed quantitatively via a non-contact optical method.[20] Photographs of specimens were captured using a 90× fixed magnification USB digital microscope (Scope Capture Digital Microscope, Guangdong, China) with an incorporated 3 MP resolution camera (U500X Capture Digital Microscope, Guangdong, China) attached to a congruent computer. The camera was placed vertically at 2.5 cm and 90° angle from each specimen. Eight adjustable LED lamps were used for illumination with a color index (R_a) close to 95%. The images were logged at 1280 × 1024 pixels and then cropped to 350 × 400 pixels. Cropped images were

https://doi.org/10.1021/acsomega.2c03745
ACS Omega 2022, 7, 34258−34267

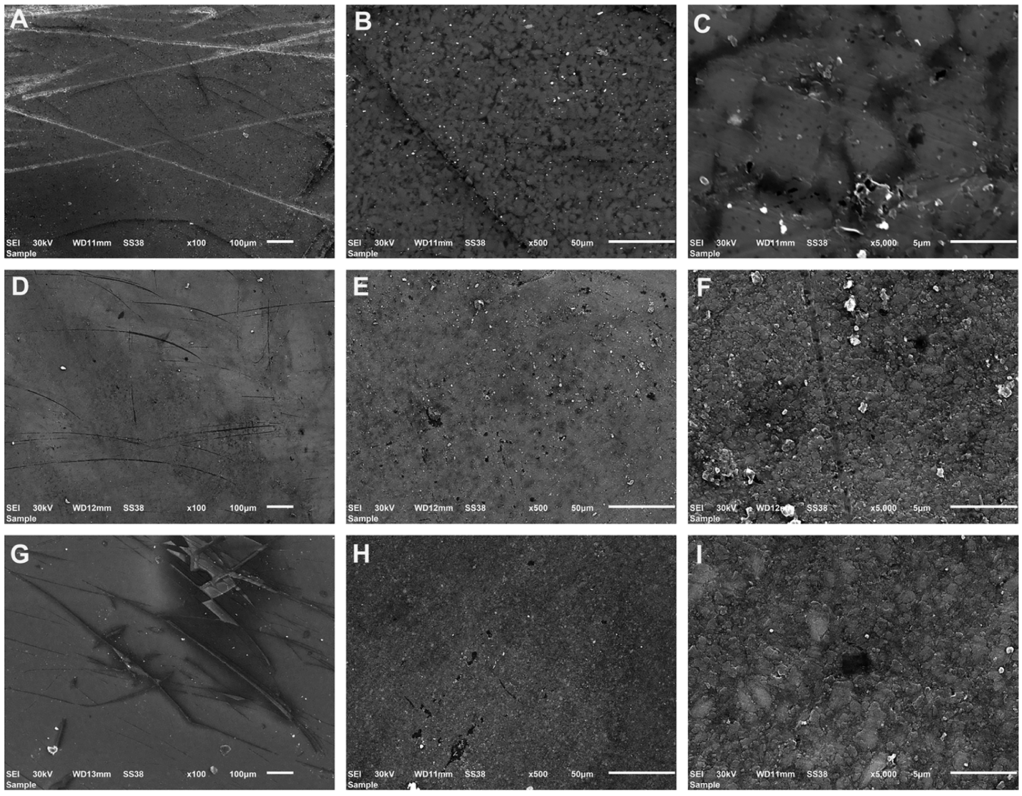

Figure 1. SEM representing the surfaces of tested CAD/CAM materials at 100×, 500×, and 5000× for Vita Enamic/VE (A, B, and C), Cerasmart/CS (D, E, and F), and Brilliant Crios/BC (G, H and I). All tested materials showed scratches on the surfaces. VE presented a smooth appearance with tightly packed irregular angular particles with sharp edges and often in clusters. Both CS and BC showed chiefly sphere-shaped particles and some irregular particles with two distinctive electro dense phases—filler phase interspersed in a matrix. BC presented soft grooves upon its surfaces and some visible hole-like round gaps or depressions.

analyzed in three dimensions (3D) using WSxM software (Ver 5 develop 4.1, Nanotec, Electronica, SL) to obtain 10 × 10 μm 3D images based on the dimension of the expected typical bacteria adherence to a restoration surface in vivo.[21,22] Conversion of pixels into absolute real-world units (μm) by the system calibration was applied to estimate the average heights (Ra) assumed as a dependable surface roughness index.[23] After the surface roughness measurement and before the biofilm formation evaluation, each specimen on both sides was sterilized under an ultraviolet wave (59S UV sterilizer; China) for 30 min.[24]

Scanning Electron Microscopy (SEM) Imaging. For imaging, one polished specimen of each group was arbitrarily elected. A scanning electron microscope (JEOL JSM-6610 LV; Akishima, Tokyo, Japan) was used to scan the gold sputter-coated specimens (Quorum Q-150R; East Sussex, BN8 6BN, United Kingdom). Images were captured using 30kv and 100×, 500×, and 5000× magnification (Figure 1).

Biofilm Formation Assay. Inoculation of both *Streptococcus mutans* and lactobacillus was carried out in a sterilized Brain heart infusion broth medium (BHI) with 7 gm/L glucose concentration (MRS), respectively, at 37 °C under anaerobic conditions for 24 h to obtain a high growth concentration of approximately 106 CFU/mL.[7] The procedure preparation started 1 day before the test. The insulated colonies of vulnerable and resistant strains were picked and grown overnight (16−18 h) or to a stationary phase (generally ∼6 h of growth) in a 5 mL of broth medium at 35−37 °C. The cultures were diluted on the test day and grew to the mid-log phase (∼1−4 h of growth). The inoculum size was standardized by measuring the absorbance at 600 nm, which was 0.5 according to the McFarland standard. While the cultures grew, the dental material discs were embedded in 8-well plate cell cultures and covered with bacterial growth, and the discs were then incubated under anaerobic conditions. The culture was left for 4 days. Later the discs were removed and transferred into sterile 5 mL tubes containing free media and shaken for about 4 h. Once the cultures were ready, 100 μL of the diluted culture were spread uniformly throughout the plate, and the excess liquid was allowed to dry. The cells were incubated overnight or permitted to grow out completely. On the following day, bacterial colonies were counted on each plate.

Cytotoxicity Procedure. *Cell Cultures.* Hep-2 cells at a concentration of (1 × 10^6 cells/mL) in culture media were procured from the VACSERA company, Giza, Egypt. Cells were grown in a MEM-E culture medium with 100 μg/mL of penicillin and 100 μg of streptomycin at 37 °C for 24 h and 95% air at 5% CO_2 until confluent monolayers were accomplished (all products: Sigma-Aldrich, Corp., St. Louis, MO, USA). The cultured cells were then preserved for more applications. A confluent sheet of Hep-2 cells was dissociated using trypsin enzyme (0.25%) for 2−3 min before being decanted. The dissociated cell was resuspended in culture media and was adjusted at a concentration of 5 × 10^4 cells/well in a 100 μL culture medium. The plates were incubated overnight. Growth medium was decanted, and serum-free medium was added to empty pre-cultured plates.

Extraction Procedure. The material under testing was collected under aseptic conditions under Laminar air flow. 10

https://doi.org/10.1021/acsomega.2c03745
ACS Omega 2022, 7, 34258−34267

mg/mL each specimen was soaked in MEM medium and incubated for 7 days at 37 °C and then cold centrifuged at 4 °C for 15 min at 4000 rpm. The supernatant was filtered using a Millipore sterile filter with a pore size of 0.22 μm.

Determination of Cytotoxic Concentrations. Tested materials were successively diluted in sterile test tubes. Various dilutions of the extraction media were attained using MEM-E medium to attain eight different concentrations.

Cytotoxicity Test Using MTT Assay. The materials' cytotoxicity was evaluated by testing the viability of cells at 24, 72, and 168 h. MTT (3-(4,5-dimethylthiazol-2-yl)-2,5-diphenyltetrazoliumbromid) is a yellow-colored tetrazolium water-soluble salt that is metabolically reduced by mitochondrial succinate dehydrogenase from viable cells and produces formazan products (blue-violet salt) accumulating in the cells. When formazan products were dissolved in alcohol, the viable cell number was correlated with calculated optical density. A direct-contact method was selected to obtain MTT cell proliferation assay (ab211091 kit, Abcam, Cambridge, UK). If cell viability is <70%, this determines the cytotoxic potential of the material.

Plates were incubated for 24 h at 37 °C and 5% CO_2. The treatment medium was decanted using phosphate buffer saline (PBS), and then, the wash buffer was decanted. After the incubation period, cell viability was evaluated utilizing MTT colorimetric assay. 50 μL MTT was added (0.5 mg/mL final concentration) to each well. The microplate was incubated for 4 h in a humidified atmosphere (37 °C, 5% CO_2). 50 μL of solubilization solution was added to each well and plated for 3−4 h at +37 °C and 5% CO_2.

Following the whole the purple formazan crystals solubilization, the absorbance of the specimens was estimated using a microplate (ELISA) reader with 570 nm wavelength. The viability % was calculated according to the following equation

$$\text{viability \%} = \frac{\text{mean OD of test dilution} \times 100}{\text{mean OD of cell control}}$$

Real Time-PCR (RT-PCR). Total RNA was extracted from control and treated Hep-2 cells utilizing the RNeasy mini kit (Qiagen-USA) per fabricator's guidelines. Using a Beckman dual spectrophotometer (Beckman-USA), the concentration and purity of extracted RNA were evaluated. The level of apoptosis-related genes was tested using RT-PCR. 10 ng of the extracted RNA of each specimen was used for cDNA synthesis using the high-capacity cDNA reverse transcriptase kit (Thermo Fischer Scientific-USA). The obtained cDNA was subsequently amplified using the Sybr Green I PCR master kit (Thermo Fisher Scientific Inc.—Lithuania) and step one apparatus (Applied Biosystems-Thermo Fischer Scientific) for 10 min at 95 °C for enzyme activation. This was followed by 40 cycles at 95 °C for 15 s, then at 55 °C for 20 s, and 72 °C for 30 s for the amplification step. Changes in the expression of the target genes were normalized compared to the mean critical threshold (CT) values of β-actin as a housekeeping gene. The specific primer sequences of genes are shown in Table 2.

Preparation of Specimens for Transmission Electron Microscopy (TEM). The wells were seeded in a 75 cm^2 cell culture flask and were treated with the tested materials for 24 h at IC50 concentration. To perform the transmission electron microscopy (TEM) analysis, the cultured media were poured, and cells were washed with PBS twice and fixed in 2.5% glutaraldehyde in phosphate buffer for 2 h at room temperature. Then, cells were washed again, and counterstaining was carried out using osmium tetroxide solution (1%) for 30 min. The fixed cells were washed with distilled water dehydrated for 10−15 min in graded ethanol concentrations (40, 60, 80, 3 × 100%), followed by propylene oxide. Then, the cells were embedded in Epon 812 (Fluka Chemie, AG, Buchs, Switzerland). Ultrathin sections (60−70 nm) by glass knives were prepared for observation using a TEM (JEOL-JEM 2100) at 80 kV. Changes in power magnification and acrosome ultrastructure were inspected from 300 sperm per specimen.

Table 2. Used Specific Primer Sequences of Genes

CYC F: 5′-CCAATGAAGATCCCACATG-3′
CYC R: 5′-CCAGGAAAGTAGGGGTTGAAGT-3′
Casp3 F: 5′-TTCATTATTCAGGCCTGCCGAGG-3′
Casp3 R: 5′-TTCTGACAGGCCATGTCATCCTCA-3′
P53 F: 5′-CCTCAGCATCTTATCCGAGTGG-3′
P53 R: 5′-TGGATGGTGGTACAGTCAGAGC-3′
β-actin F:5′-ATCGTGGGGCGCCCCAGGCAC-3′
β-actin R:5′-CTCCTTAATGTCACGCACGATTTC-3′

Statistical Analysis. Numerical data were investigated for normality by inspecting the data distribution and using normality tests (Kolmogorov−Smirnov and Shapiro−Wilk tests). All data indicated a normal (parametric) distribution. Data were presented as mean and standard deviation (SD) values. A one-way analysis of variance (ANOVA) test was utilized to compare the surface roughness, bacterial counts, and PCR results in tested groups. The significance was set at $P \leq 0.05$. Statistical analysis was conducted using software (IBM SPSS Statistics for Windows: Version 23.0; IBM Corp., Armonk, NY).

RESULTS

Surface Roughness. No statistically significant difference was obtained between mean surface roughness values in all tested groups (P-value = 0.758, effect size = 0.026), as shown in Table 3 and Figure 2.

Table 3. Descriptive Statistics and Results of a One-Way ANOVA Test for Comparison between Roughness (μm) in the Three Groups[a]

group	mean (μm)	SD	P-value	effect size (eta squared)
EN	0.2433	0.0309	0.758	0.026
CS	0.2493	0.0116		
BC	0.2371	0.0457		

[a]Significant at $P \leq 0.05$.

Biofilm Formation. The bacterial count for both *S. mutans* and *Lactobacilli* was highly significant in the BC group. Pairwise comparisons between the groups showed no significant difference between EN and CS; both revealed lower mean bacterial counts than the BC group, as shown in Table 4.

Correlation between Surface Roughness and Biofilm formation. No statistically significant correlation is observed between surface roughness and bacterial counts for all groups, as shown in Table 5.

PCR (Fold Change). As regards, Casp 3 and CYC, no statistically significant differences were calculated in pair-wise comparisons between the groups. BC and EN both showed statistically significantly lower mean fold changes than CS. While for P53, pair-wise comparisons between the groups

https://doi.org/10.1021/acsomega.2c03745
ACS Omega 2022, 7, 34258−34267

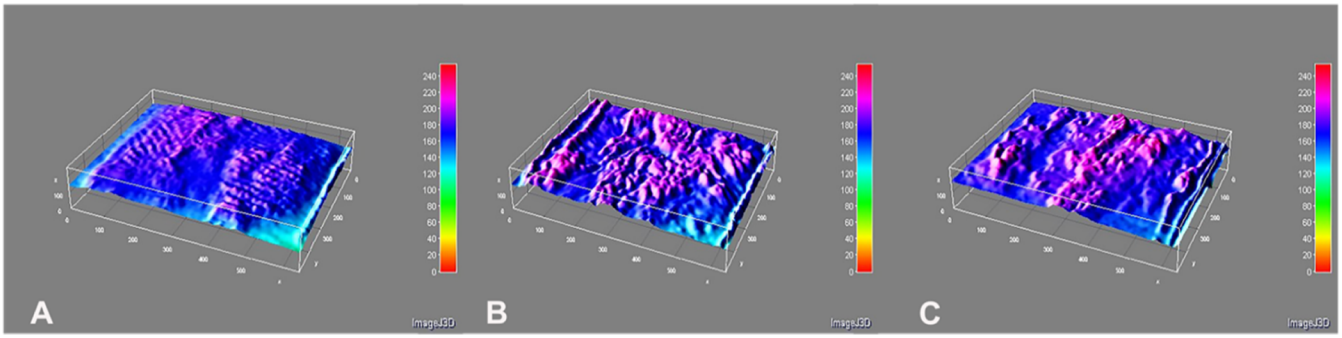

Figure 2. Representative image from 3D profilometry showing the 3D topographic surface map of EN (A), CS (B), and BC (C).

Table 4. Descriptive Statistics and Results of a One-Way ANOVA Test for Comparison between Biofilm Accumulation (CFU/mL) in the Three Groups

	EN (CFU/mL)		CS (CFU/mL)		BC (CFU/mL)			
bacteria	mean	SD	mean	SD	mean	SD	P-value	effect size (eta squared)
S. mutans	102^{B}	23.3	105.1^{B}	19.5	278.1^{A}	54.5	<0.001[a]	0.857
Lactobacilli	103.2^{B}	12	115.3^{B}	22.5	241.3^{A}	18.3	<0.001[a]	0.924

[a]Significant at $P \leq 0.05$, different superscripts indicate statistically significant differences between groups.

Table 5. Results of Pearson's Correlation Coefficient for the Correlation between Surface Roughness and Biofilm Accumulation[a]

	R_a and *S. mutans*		R_a and *Lactobacilli*	
group	correlation coefficient (r)	P-value	correlation coefficient (r)	P-value
EN	0.471	0.169	0.108	0.767
CS	0.304	0.558	−0.036	0.947
BC	0.182	0.666	0.234	0.578

[a]Significant at $P \leq 0.05$.

showed no statistically significant difference between BC and CS; both indicated significantly higher mean fold changes than EN (Table 6, Figure 3).

MTT Assay (Viability %). After 24 h, at concentrations of 5000 and 2500 μM/mL, there was a significant difference between the studied materials. Pair-wise comparisons between the groups showed the lowest cytotoxicity for EN, which has the highest mean viability %, followed by CS, while the BC group was the most cytotoxic and showed the lowest mean viability %.

After 168 h, a significant difference was calculated between the mean viability % of the three groups with different concentrations. At concentrations 10000 and 5000 μM/mL, the same cytotoxicity results were obtained; both EN and BC showed higher mean viability % with a non-significant difference. On the contrary, CS's mean viability % exhibited lower mean viability %, indicating higher cytotoxicity than previous groups. At 2500, 1250, and 625 μM/mL, the EN group showed the highest viability with no significant difference between BC and CS. At 312 μM/mL, there was no significant difference between EN and CS; both exhibited significantly higher mean viability % than BC (Figures 4 & 5).

After 168 h, there was no significant difference between the mean viability % of the three groups with different concentrations (Figure 6).

Transmission Electron Microscopy. The TEM captured the effect of different micrographs of studied materials. The reaction in cells and different organelles was described, as shown in Figure 7A–D.

DISCUSSION

Studies on resin-based composite and hybrid ceramic CAD/CAM blocks shed light on a new era of dental fixed restoration. These materials are preferred in clinical dental practice because of their ease of preparation, polishing, and reparability.[25] That is why these materials' physical aspect, antibacterial effect, and biocompatibility must be assessed. The preferred materials must have the lowest surface roughness, biofilm formation on their surfaces, and less cytotoxic and genotoxic effects.[26]

This study disclosed no correlation between the surface roughness of tested materials and biofilm formation. Many previous studies confirmed the same results.[26,27] However, other investigations showed a positive correlation.[28] Moreover, the present study revealed similar biofilm formation values for EN and CS and higher values for BC. This difference in biofilm

Table 6. Descriptive Statistics and Results of a One-Way ANOVA Test for Comparison between PCR Results (Fold Change) of the Three Groups

	EN		CS		BC			
point of comparison	mean	SD	mean	SD	mean	SD	P-value	effect size (eta squared)
casp 3	3.01^{B}	0.14	5.28^{A}	0.27	2.52^{B}	0.37	<0.001[a]	0.967
P 53	2.73^{B}	0.28	4.26^{A}	0.35	3.71^{A}	0.2	0.002[a]	0.881
CYC	3.07^{B}	0.21	7.01^{A}	0.11	3.6^{B}	0.43	<0.001[a]	0.983

[a]Significant at $P \leq 0.05$, different superscripts indicate a statistically significant difference between groups.

https://doi.org/10.1021/acsomega.2c03745
ACS Omega 2022, 7, 34258−34267

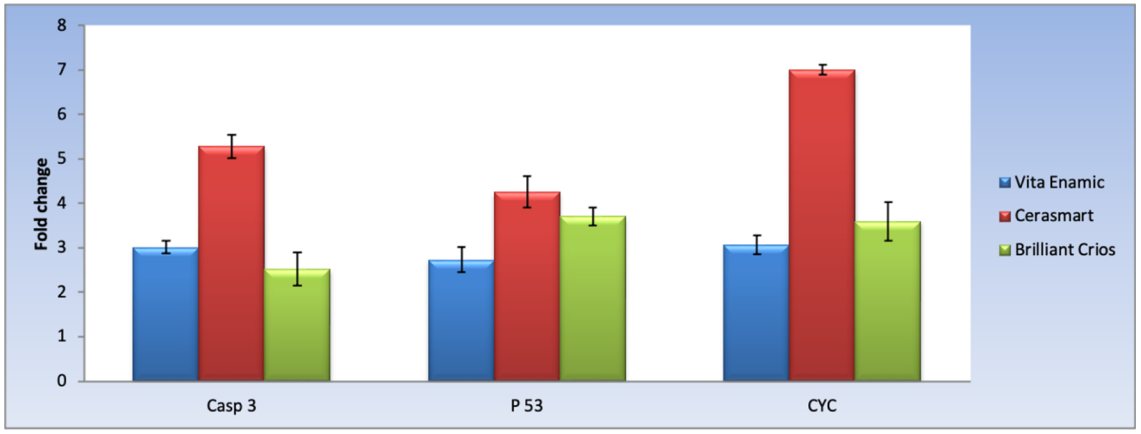

Figure 3. Bar chart representing mean and SD values for fold changes of the three groups.

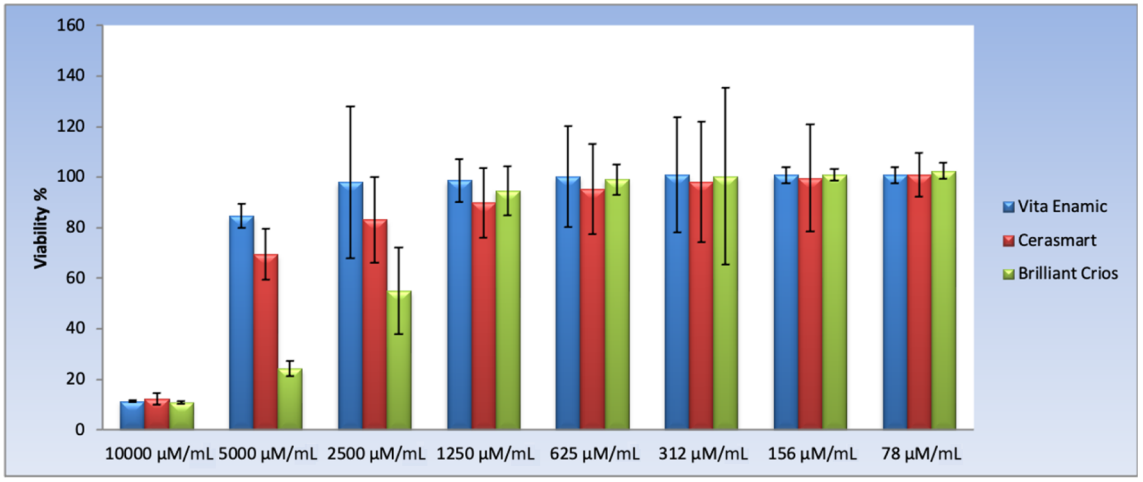

Figure 4. Bar chart representing Hep-2 cell culture showing the mean values of viability % (±SD) of all groups at different concentrations after 24 h.

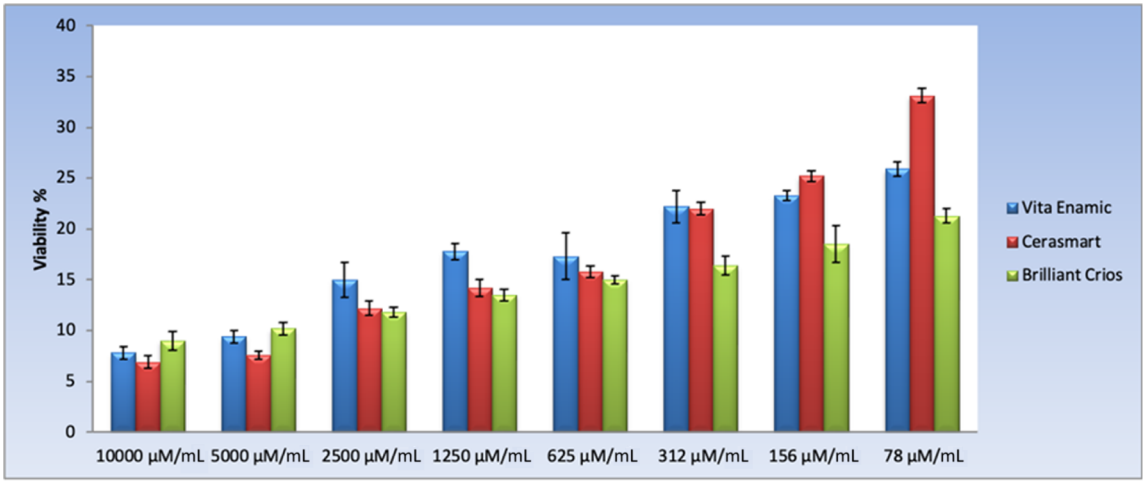

Figure 5. Bar chart representing Hep-2 cell culture showing the mean values of viability % (±SD) of all groups at different concentrations after 72 h.

formation was hard to be attributed to surface roughness due to the similarity among the three tested materials. However, the tested materials showed higher surface roughness than the threshold (0.2 μm), where no significant influence on bacterial adhesion has been reported which is still below the clinical undetectability limit of roughness (10 μm).[29,30]

Interestingly, surface topography was previously reported to have a significant difference in affecting bacterial attachment.[31,32] SEM figures of the current study revealed that BC has soft grooves upon its surfaces and some visible hole-like round gaps or depressions that may induce more biofilm adhesion (Figure 2).

https://doi.org/10.1021/acsomega.2c03745
ACS Omega 2022, 7, 34258−34267

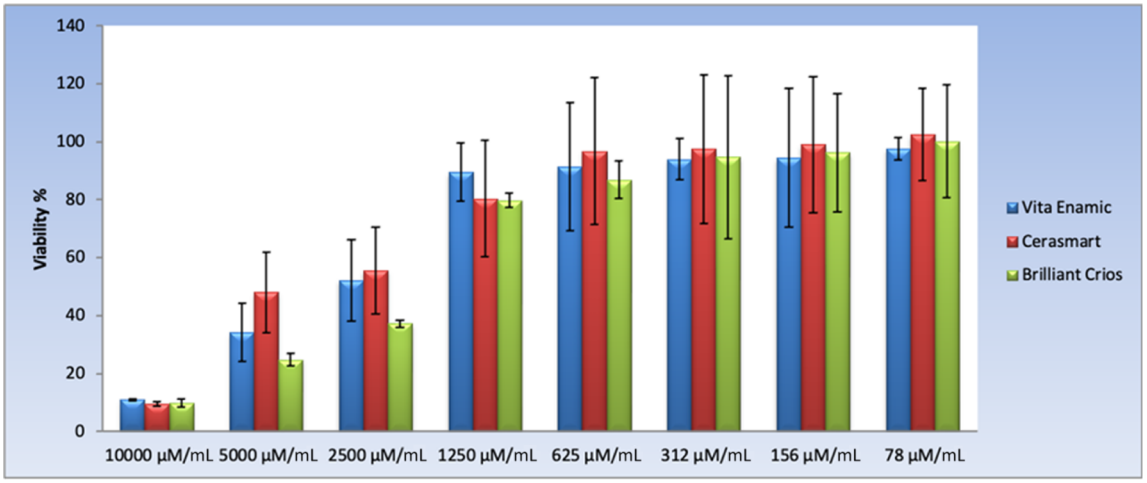

Figure 6. Bar chart representing Hep-2 cell culture showing the mean values of viability % (±SD) of all groups at different concentrations after 168 h.

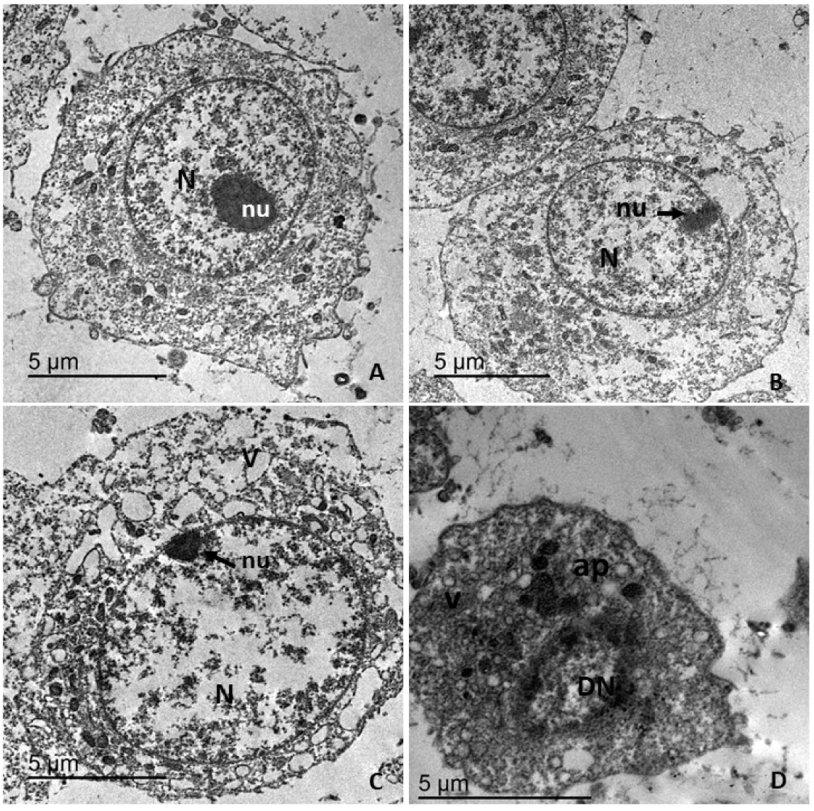

Figure 7. TEM micrographs showing control group and treated groups in Hep-2 cells. (A) Control group shows a Hep-2 cell line with a central prominent nucleus and well-detected nucleolus. (B) Cell culture group treated with EN shows the intact cell membrane and nuclear envelop. (C) Cell culture group treated with CS shows peripherally located nucleolus (nu) and vacuolated(V) cytoplasm. (D) Cell culture group treated with BC shows a disintegrated nuclear envelope, loss of chromatin material, and formation of apoptotic bodies. Shrinking of the cell membrane and accumulation of cytoplasmic vacuoles(V) are also observed.

Another critical consideration affecting biofilm creation and microbial adhesion on the dental material surfaces is the chemical composition.[28] A previous study reported that biofilm formation was positively associated with the amount of the resin matrix and negatively with the amount of the filler on the surface of the specimens. BC contains 29 wt % matrix, which is more than other tested materials.[32] Additionally, it was reported that glucosyltransferase enzymes significantly promoted the adhesion and formation activities of dental plaque biofilms.[4,33,34] Furthermore, Bis-GMA as one of the components gives a tendency of bishydroxypropoxyphenyl propane (BisHPPP), which is a biodegradation byproduct that can similarly improve the activity of *S. mutans* biofilms.[35]

In the current study, the cytotoxicity of these CAD/CAM materials was examined at different concentrations. BC recorded the highest cytotoxicity at high concentrations and the lowest for EN. The same results were obtained in previous studies.[36,37] Bakopoulou et al.[12] reported that the hydrophilic

https://doi.org/10.1021/acsomega.2c03745
ACS Omega 2022, 7, 34258−34267

monomers, HEMA in the BC composition and TEGDMA in both BC and EN, were the only monomers having the ability to diffuse at significantly high concentrations across the dentin into the pulp space. It was thought that the reason behind these results is the presence of Bis-GMA monomers, with a high degree of conversion determined as a toxic substance.[9] Another point to consider is the presence of bisphenol A in Bis-GMA, and Bis-EMA, which is also highly toxic;[38] this may support our findings of higher toxicity in the BC group, which contains both Bis-GMA and Bis-EMA.

Moreover, inconvenient with the present results, studies reported that Bis-EMA is an ethoxylated analogue of Bis-GMA due to the secondary functional (−OH) group's nonexistence. Its combination with TEGDMA results in a higher degree of conversion, decreased water solubility, and sorption. In addition, TEGDMA is more leachable into the medium, owing to its molecular structure and higher solubility than Bis-GMA. However, BC has TEGDMA while CS has not, showing a lower cytotoxic effect.[39]

Interestingly, EN showed the highest cell viability, possibly due to bisphenol's absence. Additionally, the reduced leaching of the material is attained by the controlled polymerization and strong binding of the UDMA monomer to the ceramic network. The advancement might clarify this in the polymerization mode of the material's high-temperature and high-pressure monomers and its high conversion degree.[40]

In this study, the higher viability results of CS and EN over BC may be due to it containing UDMA rather than Bis-GMA. UDMA possesses lower molecular weight, viscosity, and absence of aromatic groups over Bis-GMA, improving the toughness and decreasing the monomer release, resulting in less cytotoxicity. This might be explained by the severe cytotoxicity of BC over the other studied materials.[41]

In BC and CS, the significant elevation of p53 fold change in response to DNA damage ensures the genotoxic effect of these materials if compared to EN. However, no significant difference was declared between the two groups.

It is well established that monomers are reported to induce bacterial colonization on the composite surface, pulp damage, and cytotoxic and genotoxic effects as negative effects.[42] The manufacturing technique in CAD/CAM materials may explain the difference in the leaching pattern of monomers in contrast to conventional composite resins. This was explained as those materials were pre-polymerized into blocks and thus resulted in improved chemical properties, leading to decreased monomers leaching over time.[43]

Genotoxicity is the agent's ability to interact with genetic material inducing DNA damage. Several methodologies are commonly used to detect genetic damage and mutations in various endpoints, including DNA strand breaks, chromosome translocations, chromosomal loss, point mutations, or spindle cell apparatus interference.[44] It was reported that the dysfunction of many genes coding for anti-apoptotic proteins, transcription factors, and tumor suppressors is the cause of most cancers. These genes can be targeted for the treatment of cancer.[45]

The p53 tumor suppressor gene encodes a nuclear phosphoprotein with cancer inhibiting properties mutated in more than 50% of human cancers. Many genotoxic stresses induce the p53 protein. p53 mutation patterns in human cancers are assumed to reflect the effects of the specific carcinogens.[45,46]

This present study evaluated the role of P53, caspase-3, and cytochrome *C* and measured the expression levels of apoptosis regulatory genes on the three different studied materials. In CS and BC, the p53 showed significantly high levels than that in the EN, indicating the lowest genotoxicity.

This study revealed that tested materials have an apoptotic effect on Hep-2 cells. RT-PCR analysis of pro and anti-apoptotic gene expression levels demonstrated that the lowest expression was for EN type. The same results were obtained in MTT and TEM sections that reveal minimal cellular changes. The investigations also proved that fold change in the CS group was the highest, and the difference was significant in cytochrome *C* and caspase-3. Interestingly, this group showed nuclear and cytoplasmic changes in ultrastructure, as shown in the TEM sections.

In agreement with these findings, caspase activation is involved in initiating DNA damage, which leads to apoptosis.[47] Moreover, this activation is regulated by different triggers, like death receptors and mitochondria disruption. The disruption is activated by cellular stresses, growth factor deprivation, cytoskeletal disruption, and DNA damage.[48] This results in leakage of cytochrome *C* and downregulation of anti-apoptotic protein. This also proves the role of caspases-3 as a major factor in DNA damage.[49]

Huang et al.[47] reported that TEGDMA could induce activations of caspases-3, 28, and 29. This could be explained that the mitochondria might be directly disrupted by TEGDMA, which passes through the cell membrane and causes cellular stresses and then excessive reactive oxygen species (ROS) production. However, According to Lovász et al., TEGDMA exposure significantly increased caspase-3 and caspase-8 and cleaved caspase-9 levels.[49] The induction of ROS production has been confirmed to be one of the chief monomer toxicity mechanisms.[47,50,51] Moreover, ROS has exhibited an effect in the activation of intrinsic and extrinsic caspase-dependent apoptotic pathways.[52]

Furthermore, concerning genotoxicity, Bis-GMA and UDMA have increased the micronuclei number as TEGDMA and HEMA do. In addition, it was shown that these monomers induced DNA migration.[53]

Bakopoulou concluded that the basic resinous monomers Bis-GMA and UDMA might significantly contribute to tested resin-based materials' cytotoxicity and genotoxicity.[12] Besides, due to their hydrophobic property, which confines their release into aqueous environments, they can apply their cytotoxicity at lower concentrations than HEMA and TEGDMA monomers.

Generally, the cytotoxicity depends on the materials' monomer composition, which is ranked as Bis-GMA > UDMA > TEGDMA > HEMA.[54] In conformity with the current study, it has been informed that dental composite resins can release compounds with severe (Bis-GMA, TEGDMA, UDMA, *και* DMDTA, and DMBZ) or medium (HEMA, BEMA, DMAPE, DMPT, and CQ) cytotoxic effect.[54]

CONCLUSIONS

The investigated CAD/CAM blocks showed no significant difference in surface roughness. Moreover, no correlation was shown between the surface roughness and biofilm formation. Considering cytotoxicity, BC showed the highest values, followed by CS and EN. Consequently, EN was considered the most biocompatible material among the tested ones.

https://doi.org/10.1021/acsomega.2c03745
ACS Omega 2022, 7, 34258−34267

AUTHOR INFORMATION

Corresponding Author

Yasmine Alaa El-din − *Lecturer of Oral & Maxillofacial Pathology, Faculty of Dentistry, October 6 University, Giza 12511, Egypt*; orcid.org/0000-0003-4435-6829; Phone: 00201003790332; Email: yasminealaaeldin.dent@o6u.edu.eg

Authors

Soha A. Hassan − *Associate Professor of Cell Biology and Genetics Faculty of Dentistry-October 6 University, Giza 12511, Egypt*

Marwa Beleidy − *Lecturer of Fixed Prosthodontics, Faculty of Dentistry, October 6 University, Giza 12511, Egypt*

Complete contact information is available at: https://pubs.acs.org/10.1021/acsomega.2c03745

Author Contributions

All authors had substantial contributions to conception, design, acquisition of data, analysis, interpretation of data, the drafting of the manuscript, and critical revision and final approval for its intellectual content.

Notes

The authors declare no competing financial interest.

ACKNOWLEDGMENTS

We want to thank Dr. Khaled Mohamed Keraa, Biostatistician, Quality Management Specialist Faculty of Oral and Dental Medicine, Misr International University (MIU)—Egypt for his great efforts in statistics of this manuscript.

REFERENCES

(1) Giordano, R. Materials for chairside CAD/CAM-produced restorations. *J. Am. Dent. Assoc., JADA* **2006**, *137*, 14S−21S.

(2) Spitznagel, FA.; Scholz, KJ.; Vach, K.; Gierthmuehlen, P. C. Monolithic polymer- infiltrated ceramic network CAD/CAM single crowns: three-years mild-term results of a prospective clinical study. *Int. J. Prosthod.* **2020**, *33*, 160−168.

(3) Cinar, S.; Altan, B.; Akgungor, G. Comparison of bond strength of monolithic CAD-CAM materials to resin cement using different surface treatment methods. *J. Adv. Oral Res.* **2019**, *10*, 120−127.

(4) Ionescu, R. N.; Totan, A. R.; Imre, M. M.; Ţâncu, A. M. C.; Pantea, M.; Butucescu, M.; Farcaşiu, A. T. Prosthetic Materials Used for Implant-Supported Restorations and Their Biochemical Oral Interactions: A Narrative Review. *Materials* **2022**, *15*, 1016.

(5) Awada, A.; Nathanson, D. Mechanical properties of resin-ceramic CAD/CAM restorative materials. *J. Prosthet. Dent.* **2015**, *114*, 587−593.

(6) Alamoush, R. A.; Silikas, N.; Salim, N. A.; Al-Nasrawi, S.; Satterthwaite, J. D. Effect of the composition of CAD/CAM composite blocks on mechanical properties. *BioMed Res. Int.* **2018**, *2018*, 4893143.

(7) Skorulska, A.; Piszko, P.; Rybak, Z.; Szymonowicz, M.; Dobrzyński, M. Review on Polymer, Ceramic and Composite Materials for CAD/CAM Indirect Restorations in Dentistry—Application, Mechanical Characteristics and Comparison. *Materials* **2021**, *14*, 1592.

(8) Nashaat, Y.; Sabry, H.; Hassan, S. A. Evaluation of the Cytotoxicity and apoptotic effect of Nano triple antibiotic paste with Nano anti-inflammatory drug as an intracanal medicament. *Eur. Endod. J.* **2021**, *6*, 82−89.

(9) Pituru, S. M.; Greabu, M.; Totan, A.; Imre, M.; Pantea, M.; Spinu, T.; Tancu, A. M.; Popoviciu, N. O.; Stanescu, I. I.; Ionescu, E. A Review on the Biocompatibility of PMMA-Based Dental Materials for Interim Prosthetic Restorations with a Glimpse into their Modern Manufacturing Techniques. *Materials* **2020**, *13*, 2894.

(10) Gautam, R.; Singh, R. D.; Sharma, V. P.; Siddhartha, R.; Chand, P.; Kumar, R. Biocompatibility of polymethylmethacrylate resins used in dentistry. *J. Biomed. Mater. Res., Part B* **2012**, *100B*, 1444−1450.

(11) Holban, A.-M.; Farcasiu, C.; Andrei, O.-C.; Grumezescu, A. M.; Farcasiu, A.-T. Surface Modification to Modulate Microbial Biofilms—Applications in Dental Medicine. *Materials* **2021**, *14*, 6994.

(12) Bakopoulou, A.; Papadopoulos, T.; Garefis, P. Molecular toxicology of substances released from resin-based dental restorative materials. *Int. J. Mol. Sci.* **2009**, *10*, 3861−3899.

(13) Ribeiro, D.; Yujra, V.; DE Moura, C.; Handan, B.; DE Barros Viana, M.; Yamauchi, L.; Castelo, P.; Aguiar, O. Genotoxicity Induced by Dental Materials: A Comprehensive Review. *Anticancer Res.* **2017**, *37*, 4017−4024.

(14) Ferracane, J. L. Current trends in dental composites. *Crit. Rev. Oral Biol. Med.* **1995**, *6*, 302−318.

(15) Durner, J.; Spahl, W.; Zaspel, J.; Schweikl, H.; Hickel, R.; Reichl, F. X. Eluted substances from unpolymerized and polymerized dental restorative materials and their Nernst partition coefficient. *Dent. Mater.* **2010**, *26*, 91−99.

(16) Andrioli, N. B.; Chaufan, G.; Coalova, I.; Molina, M. D. C.; Mudry, M. D. HEP-2 Cell Line As An Experimental Model To Evaluate Genotoxic Effects Of Pentavalent Inorganic Arsenic. *BAG* **2017**, *2*, 15−24.

(17) Coalova, I.; Ríos de Molina, M. C.; Chaufan, G. Influence of the spray adjuvant on the toxicity effects of a glyphosate formulation. *Toxicol. Vitro* **2014**, *28*, 1306−1311.

(18) Aydın, N.; Karaoglanoglu, S.; Oktay, E. A. Evaluating Cytotoxic Effects of Resin Based CAD/CAM Blocks. *J. Res. Med. Dent. Sci.* **2020**, *8*, 131−136.

(19) Abu-Obaid, A.; AlMawash, N.; Alyabis, N.; Alzaaqi, N. An in vitro evaluation of the effect of polishing on the stainability of different CAD/CAM ceramic materials. *Saudi Dent. J.* **2020**, *32*, 135−141.

(20) Abouelatta, O. B. 3D Surface Roughness Measurement Using a Light Sectioning Vision System. *Proc. World Congr. Eng.* **2010**, *1*, 698−703.

(21) Horcas, I.; Fernández, R.; Gómez-Rodríguez, J. M.; Colchero, J. W.; Gómez-Herrero, J. W.; Baro, A. M. WSXM: A software for scanning probe microscopy and a tool for nanotechnology. *Rev. Sci. Instrum.* **2007**, *78*, 013705.

(22) Giacomelli, L.; Derchi, G.; Frustaci, A.; Bruno, O.; Covani, U.; Barone, A.; De Santis, D.; Chiappelli, F. Surface Roughness of Commercial Composites after Different Polishing Protocols: An Analysis with Atomic Force Microscopy. *Open Dent. J.* **2010**, *4*, 191−194.

(23) Kakaboura, A.; Fragouli, M.; Rahiotis, C.; Silikas, N. Evaluation of surface characteristics of dental composites using profilometry, scanning electron, atomic force microscopy, and gloss-meter. *J. Mater. Sci. Mater. Med.* **2007**, *18*, 155−163.

(24) Lee, J.-H.; Jun, S.-K.; Moon, H.-J.; Lee, H.-H. Cytotoxicity and proinflammatory cytokine expression induced by interim resin materials in primary cultured human dental pulp cells. *J. Prosthet. Dent.* **2017**, *118*, 524−534.

(25) Ruse, N. D.; Sadoun, M. J. Resin-composite blocks for dental CAD/CAM applications. *J. Dent. Res.* **2014**, *93*, 1232−1234.

(26) Aykent, F.; Yondem, I.; Ozyesil, AG.; Gunal, SK.; Avunduk, MC.; Ozkan, S. Effect of different finishing techniques for restorative materials on surface roughness and bacterial adhesion. *J. Prosthet. Dent.* **2010**, *103*, 221−227.

(27) Pereira, C. A.; Eskelson, E.; Cavalli, V.; Liporoni, P. C.; Jorge, A. O.; Rego, M. A. Streptococcus mutans biofilm adhesion on composite resin surfaces after different finishing and polishing techniques. *Operat. Dent.* **2011**, *36*, 311−317.

(28) Yuan, C. X.; Wang, X.; Gao, F.; Chen, X.; Liang, D.; Li, D. Effects of surface properties of polymer- based restorative materials on early adhesion of Streptococcus mutans in vitro. *J. Dent.* **2016**, *54*, 33−40.

(29) Kawai, K.; Urano, M.; Ebisu, S. Effect of surface roughness of porcelain on adhesion of bacteria and their synthesizing glucans. *J. Prosthet. Dent.* **2000**, *83*, 664−667.
(30) Kilic, K.; Kesim, B.; Sumer, Z.; Polat, Z.; Kesim, S. In vitro cytotoxicity of all-ceramic sub structural materials after aging. *J. Dent. Sci.* **2013**, *8*, 231−238.
(31) Quirynen, M.; Bollen, C. M. The influence of surface roughness and surface-free energy on supra- and subgingival plaque formation in man. A review of the literature. *J. Clin. Periodontol.* **1995**, *22*, 1−14.
(32) Lourenço, B. N.; Marchioli, G.; Song, W.; Reis, RL.; van Blitterswijk, CA.; Karperien, M.; van Apeldoorn, A.; Mano, J. F. Wettability influences cell behavior on super- hydrophobic surfaces with different topographies. *Biointerphases* **2012**, *7*, 46.
(33) Kawai, K.; Tsuchitani, Y. Effects of resin composite components on glucosyltransferase of cariogenic bacterium. *J. Biomed. Mater. Res.* **2000**, *51*, 123−127.
(34) Brambilla, E.; Gagliani, M.; Ionescu, A.; Fadini, L.; García-Godoy, F. The influence of light-curing time on the bacterial colonization of resin composite surfaces. *Dent. Mater.* **2009**, *25*, 1067−1072.
(35) Kilic, K.; Kesim, B.; Sumer, Z.; Polat, Z.; Kesim, S. In vitro cytotoxicity of all-ceramic substructural materials after aging. *J. Dent. Sci.* **2013**, *8*, 231−238.
(36) Delaviz, Y.; Finer, Y.; Santerre, J. P. Biodegradation of resin composites and adhesives by oral bacteria and saliva: A rationale for new material designs that consider the clinical environment and treatment challenges. *Dent. Mater.* **2014**, *30*, 16−32.
(37) Grenade, C.; De Pauw-Gillet, MC.; Pirard, C.; Bertrand, V.; Charlier, C.; Vanheusden, A.; Mainjot, A. Biocompatibility of polymer-infiltrated-ceramic-network (PICN) materials with Human Gingival Keratinocytes (HGKs). *Dent. Mater.* **2017**, *33*, 333−343.
(38) Mourouzis, P.; Samanidou, V.; Palaghias, G. HPLC study of the inhibiting effect of phosphate and bicarbonate buffers on the leaching pattern of dental resin composites. *J. Liq. Chromatogr. Relat. Technol.* **2018**, *41*, 196−202.
(39) Colotta, F.; Allavena, P.; Sica, A.; Garlanda, C.; Mantovani, A. Cancer-related inflammation, the seventh hallmark of cancer: links to genetic instability. *Carcin* **2009**, *30*, 1073−1081.
(40) Krifka, S.; Spagnuolo, G.; Schmalz, G.; Schweikl, H. A review of adaptive mechanisms in cell responses towards oxidative stress caused by dental resin monomers. *Biomaterials* **2013**, *34*, 4555−4563.
(41) Floyd, C. J. E.; Dickens, S. H. Network structure of Bis-GMA and UDMA-based resins systems. *Dent. Mater.* **2007**, *22*, 1143−1149.
(42) Gupta, S.; Saxena, P.; Pant, V.; Pant, A. Release and toxicity of dental resin composite. *Toxicol. Int.* **2012**, *19*, 225−234.
(43) Ribeiro, DA.; Yujra, V. Q.; De Moura, C. F. G.; Handan, B. A.; DE Barros Viana, M. D. B.; Yamauchi, L.; Castelo, P.; Aguiar, O. Genotoxicity Induced by Dental Materials: A Comprehensive Review. *Anticancer Res.* **2017**, *37*, 4017−4024.
(44) Frederik, I. H.; Krammer, P. H. Death and anti-death: tumour resistance to apoptosis. *Nat. Rev. Cancer* **2002**, *2*, 277−288.
(45) Rivlin, N.; Brosh, R.; Oren, M.; Rotter, V. Mutations in the p53 Tumour Suppressor Gene. Important Milestones at the Various Steps of Tumorigenesis. *Genes Cancer* **2011**, *2*, 466−474.
(46) Decordier, I.; Cundari, E.; Kirsch-Volders, M. Survival of aneuploid, micronucleated and/or polyploid cells: Crosstalk between ploidy control and apoptosis. *Mutat. Res.* **2008**, *651*, 30−39.
(47) Huang, F. M.; Kuan, Y. H.; Lee, S. S.; Chang, Y. C. Cytotoxicity and genotoxicity of triethyleneglycol-dimethacrylate in macrophages involved in DNA damage and caspases activation. *Environ. Toxicol.* **2015**, *30*, 581−588.
(48) Brenner, D.; Mak, T. W. Mitochondrial cell death effectors. *Curr. Opin. Cell Biol.* **2009**, *21*, 871−877.
(49) Lovász, B. V.; Berta, G.; Lempel, E.; Sétáló, G.; Vecsernyés, M.; Szalma, J. TEGDMA (Triethylene Glycol Dimethacrylate) Induces Both Caspase-Dependent and Caspase-Independent Apoptotic Pathways in Pulp Cells. *Polymers* **2021**, *13*, 699.
(50) Eckhardt, A.; Gerstmayr, N.; Hiller, K. A.; Bolay, C.; Waha, C.; Spagnuolo, G.; Camargo, C.; Schmalz, G.; Schweikl, H. TEGDMA-induced oxidative DNA damage and activation of ATM and MAP kinases. *Biomaterials* **2009**, *30*, 2006−2014.
(51) Yeh, C. C.; Chang, J. Z.; Yang, W. H.; Chang, H. H.; Lai, E. H.; Kuo, M. Y. NADPH oxidase 4 is involved in the triethylene glycol dimethacrylate-induced reactive oxygen species and apoptosis in human embryonic palatal mesenchymal and dental pulp cells. *Clin. Oral Invest.* **2015**, *19*, 1463−1471.
(52) Elmore, S. Apoptosis: A review of programmed cell death. *Toxicol. Pathol.* **2007**, *35*, 495−516.
(53) Kleinsasser, N. H.; Schmid, K.; Sassen, A. W.; Harréus, U. A.; Staudenmaier, R.; Folwaczny, M.; Glas, J.; Reichl, F. X. Cytotoxic and genotoxic effects of resin monomers in human salivary gland tissue and lymphocytes as assessed by the single cell microgel electrophoresis (comet) assay. *Biomaterials* **2006**, *27*, 1762−1770.
(54) Reichl, F. X.; Esters, M.; Simon, S.; Seiss, M.; Kehe, K.; Kleinsasser, N.; Folwaczny, M.; Glas, J.; Hickel, R. Cell death effects of resin-based dental material compounds and mercurials in human gingival fibroblasts. *Arch. Toxicol.* **2006**, *80*, 370−377.

https://doi.org/10.1021/acsomega.2c03745
ACS Omega 2022, 7, 34258−34267